Enhancement of cortical network activity *in vitro* and promotion of GABAergic neurogenesis by stimulation with an electromagnetic field with a 150 MHz carrier wave pulsed with an alternating 10 and 16 Hz modulation

Alexandra Gramowski-Voß[1]*, Hans-Joachim Schwertle[1], Anna-Maria Pielka[2], Luise Schultz[1,2], Anne Steder[1], Konstantin Jügelt[1], Jürgen Axmann[3] and Wolfgang Pries[4]

[1] *Division of Electrophysiology, NeuroProof GmbH, Rostock, Germany,* [2] *Division of Molecular Biology, NeuroProof GmbH, Rostock, Germany,* [3] *Engineering Office for Bioresonance and Environmental Technology, Werder/Havel, Germany,* [4] *Megawave GmbH, Bad Wörishofen, Germany*

In recent years, various stimuli were identified capable of enhancing neurogenesis, a process which is dysfunctional in the senescent brain and in neurodegenerative and certain neuropsychiatric diseases. Applications of electromagnetic fields to brain tissue have been shown to affect cellular properties and their importance for therapies in medicine is recognized. In this study, differentiating murine cortical networks on multiwell microelectrode arrays were repeatedly exposed to an extremely low-electromagnetic field (ELEMF) with alternating 10 and 16 Hz frequencies piggy backed onto a 150 MHz carrier frequency. The ELEMF exposure stimulated the electrical network activity and intensified the structure of bursts. Further, the exposure to electromagnetic fields within the first 28 days *in vitro* of the differentiation of the network activity induced also reorganization within the burst structure. This effect was already most pronounced at 14 days *in vitro* after 10 days of exposure. Overall, the development of cortical activity under these conditions was accelerated. These functional electrophysiological changes were accompanied by morphological ones. The percentage of neurons in the neuron glia co-culture was increased without affecting the total number of cells, indicating an enhancement of neurogenesis. The ELEMF exposure selectively promoted the proliferation of a particular population of neurons, evidenced by the increased proportion of GABAergic neurons. The results support the initial hypothesis that this kind of ELEMF stimulation could be a treatment option for specific indications with promising potential for CNS applications, especially for degenerative diseases, such as Alzheimer's disease and other dementias.

Keywords: extremely low-electromagnetic field, cortical networks, neurogenesis, multiwell microelectrode recording, phenotypic screening, functional biomarker

Abbreviations: AD, Alzheimer's disease; CNS, central nervous system; CV, coefficient of variation; Div, days *in vitro*; DMEM, Dulbecco's modified Eagle's medium; EEG, electroencephalography; ELEMF, extremely low-electromagnetic field; GABA, gamma-aminobutyric acid; MEA, microelectrode array; MRI, magnetic resonance imaging; NIH, National Institute of Health; PTZ, pentylenetetrazole; SEM, standard error of mean.

Introduction

Already in 1896, Virchow expressed the modern idea in the context of regulation and disease: "The disease begins in the moment when the regulatory apparatus of the body is insufficient to eliminate the interference. Not life under abnormal conditions, not the disorder as such produces disease, but the disease begins with the insufficiency of the regulatory apparatuses" (1). In this respect, an increasing body of literature indicates that electrical and magnetic fields interact significantly with biological systems (2–6). Magnetic and electromagnetic fields (EMFs) are recognized by present-day medicine as real physical entities that could contribute to the healing of various health problems, e.g., pain treatment (7, 8). Electromagnetic therapies are well known and successful in medicine. Proposed and modeled mechanisms are, e.g., ion cyclotron resonance, ion parametric resonance (9, 10), free radicals (11), and the activation of heat shock proteins. One of the first electrochemical models proposed that the cell membrane exerts linear physicochemical changes (12, 13) to assess the EMF parameters for which biological effects might be expected. It was assumed that non-thermal EMF may directly affect ion binding and/or transport, and possibly alter the cascade of biological processes related to tissue growth and repair (4, 6, 14). However, the transduction mechanism for non-thermal EMF biological effects has not been fully elucidated. It is thought that the effectiveness is related to the fine manipulation of cell regulation and communication taking place in this power range.

In recent years, several studies identified various stimuli capable of enhancing neurogenesis in adults, a process, which is dysfunctional in the senescent brain as well as in neurodegenerative and neuropsychiatric diseases. EMFs were already applied in several clinical studies. Saitoh and co-workers demonstrated in a randomized, multicenter, double-blind, crossover, sham-controlled clinical study that daily repeated 5-Hz transcranial magnetic stimulation of primary cortex provided short-term pain relief in neuropathic pain patients (15, 16). They also confirmed that high-frequency transcranial magnetic stimulation over the M1 food area significantly improved motor symptoms in patients with Parkinson's disease (17). Pries and Baumgart (18) showed in a MRT study that treating patients with knee osteoarthritis twice a day for 60 min for eight consecutive days with exposure to 150 MHz fields pulsed with 10 Hz decreased knee contusion and recovered knee cartilage.

Following up on these reports, we addressed in this study the possible involvement of basic modifications caused by alternating magnetic stimulation by determining functional phenotypic as well as morphological cellular changes. We investigated the effects of repeated exposures to 150 MHz stimulation with pulsed 10 and 16 Hz modulation on the developmental growth of primary cortical networks cultured on microelectrode arrays (MEAs) and their neuronal network activity by an electrophysiological multichannel recording assay. Unlike so-called target-based assays for tests of biological effects on individual receptors or target proteins, functional assays using primary cultures of neural networks on MEAs provide a reflection of the central nervous system with its complex multicellular interconnections. They allow phenotypic screening, which are demonstrably more successful in drug development than target-based approaches (19–22). The MEA neurochip technology is a sophisticated phenotypic high-content screening method to characterize functional changes in network activity in electrically active cell cultures and it is very sensitive to neurogenesis, as well as neuroregenerative and -degenerative aspects (22–28, 29).

Materials and Methods

Primary Cortical Cell Cultures

Experiments were carried out in accordance with the EU Directive 2010/63/EU on the protection of animals used for scientific purposes (certification file number 7221.3-2). As previously described (26, 30), embryonic frontal tissues were harvested from E 15 NMRI mice (Charles River, Sulzfeld, Germany). Frontal cortex was dissociated enzymatically in DMEM10/10 (10% horse and 10% fetal calf serum) including papain and DNase I, and mechanically with transfer pipettes. The cells were resuspended in DMEM10/10 at a density of 1.0×10^6 cells/ml, and 300 µl were seeded onto each well of 12-well MEA neurochips (Axion Biosystems Inc., Atlanta, GA, USA). Each well contains an array of 64 embedded platinum electrodes resulting in a total of 768 channels. As non-electronic reference 24 well plates with 13 mm cover slips were plated with 100 µl at a density of 1.5×10^6 cells/ml. For better adhesion, the neurochips were coated with poly-D-lysine and laminin before the preparation to ensure cell attachment within a confined adhesive region (5 mm diameter centered around the electrode area). Cultures were kept at 37°C in a 10% CO_2 atmosphere for 4 weeks and fed twice a week with DMEM containing 10% horse serum (**Figure 1A**). The developing co-cultures were treated at day 5 *in vitro* with 5-fluoro-2′-deoxyuridine to prevent glial proliferation and overgrowth.
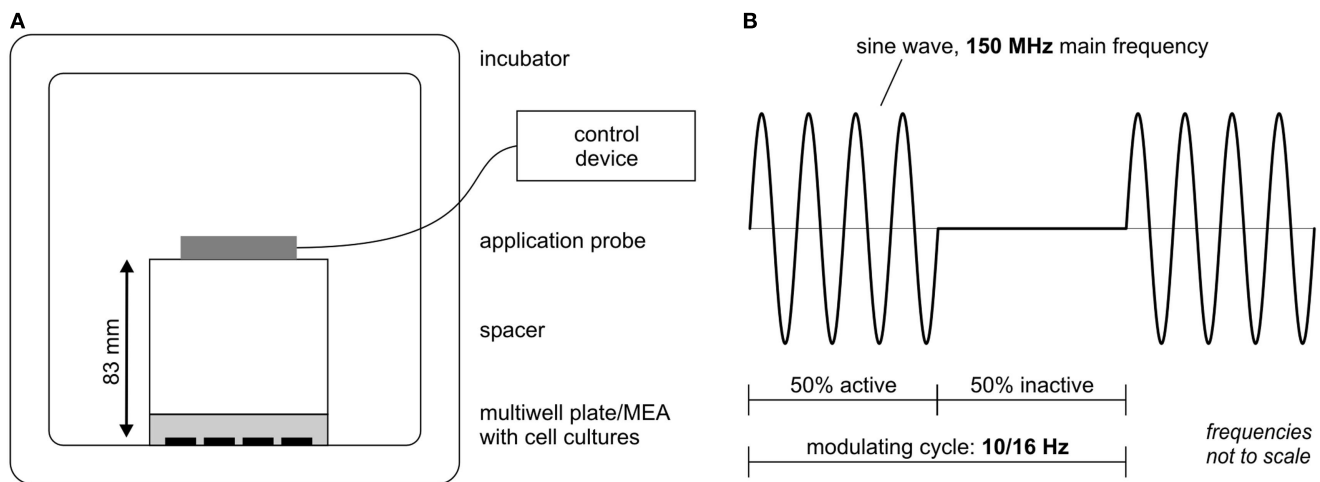
Alternating Magnetic Field Stimulation

The extremely low electromagnetic field (ELEMF) signal used in this study was generated by the stimulation device MegaWave MW150 (MegaWave GmbH, Bad Wörishofen, Germany), which is an accredited medicine product according to the medicine product guideline 93/42/EWG. It has a high-frequency oscillator stage that generates a fixed carrier frequency of 150 MHz. A low-frequency oscillator stage generates an adjustable lower frequency as the modulation frequency. Settings used in this study are depicted in **Figure 2**. The stimulation parameters as well as the distance between cortical cultures and stimulation probe were chosen from pilot study data (data not shown). The durations of the cycles were set to 100 or 62.5 ms (equivalent to 10 or 16 Hz) with modulation setting to 50% cycle time. The 50% stimulation rhythm (50 or 31.25 ms) was followed by 50% silence phase (50 or 31.25 ms) (**Figure 2B**). The power level was set to 3 resulting in a power output of 0.240 mW ± 15%. The magnetic induction pulses at the applied settings equaled a maximum magnetic flux density of 0.125 pT (125 E-15 Vs/m²). The distance between the applicator probe (cross section diameter 70 mm) and the cortical cultures was set to 83 mm (**Figure 2A**). Plastic ware empty multiwell plates were used as spacer. The cortical network cultures on Axion 12-well MEAs and 24-well plates were successively exposed from 4 to 28 days *in vitro* twice a week in a designated
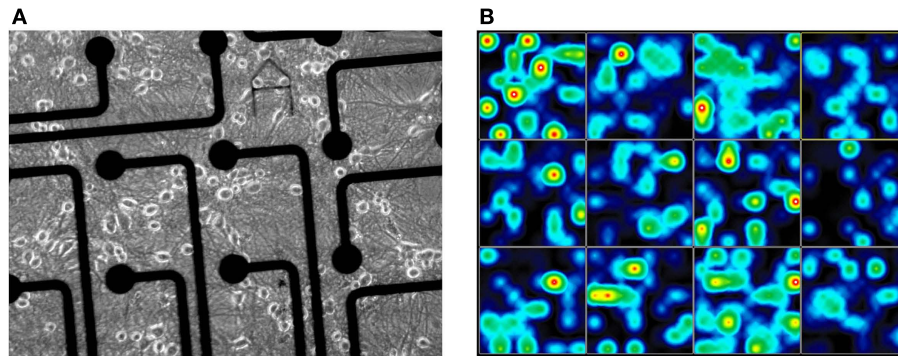
FIGURE 1 | Multichannel electrophysiological Axion electrode array of the 12-well plate for extracellular recording of cortical network activity. (A) Electrode area with cortical culture at 12 days *in vitro* (scale: 30 µm electrode diameter); (B) Spike activity heat map of frontal cortex activity (28 div) cultures in an Axion 12-well MEA with 64 electrodes per well.

FIGURE 2 | Extremely low-electromagnetic field exposure set up scheme. (A) Experimental stimulation set up in the incubator. (B) Waveform scheme of the extremely low-electromagnetic field studied here: a 150-MHz carrier frequency signal is pulse modulated with 50% time modulation burst (100 or 62.5 ms) repeated for modulating frequencies 10 and 16 Hz.

incubator under constant conditions (10% CO_2, 37°C) first to 30 min of a modulating frequency of 10 Hz followed by 30 min at 16 Hz. The control group (separate Axion 12-well MEAs and 24-well plates) was handled with the same procedure, except for the EMF exposure.

Multichannel Recording

In principle, electrophysiological studies were performed as described by Gramowski et al. (26). Recordings were executed with the Maestro recording system by Axion Biosystems Inc. (Atlanta, GA, USA) providing 1200× amplification, sampling at 12.5 kHz, filtering, and spike detection, delivering whole channel neuronal spike data. For extracellular recordings, MEAs were maintained at 37°C and a pH of 7.4 through a continuous filtered and humidified airflow with 10% CO_2. Recordings were made in DMEM with 10% horse serum. The network response was recorded for at least 1 h

(**Figure 1B**). The neuronal networks were recorded after 14 and 28 days *in vitro*, respectively.

Multiparametric Data Analysis

Each unit represents the activity originating from one neuron recorded at one electrode. Units are separated at the beginning of the recording. We analyzed the stable activity phase of the last 30 min. Action potentials (spikes) were recorded as spike trains, which are clustered in so-called bursts. Bursts were quantified via direct spike train analysis using the standard interspike interval (ISI) method in NPWaveX (NeuroProof GmbH, Rostock, Germany). Bursts are defined by the following parameters: maximum ISI to start a burst: 40 ms, minimum ISI to end a burst: 200 ms, minimum interval between bursts: 100 ms, minimum duration of burst: 10 ms, and min number of spikes in a burst: 2.

With a multiparametric high-content analysis of the network activity patterns, we extract 204 activity-describing spike train parameters and thereby obtain a precise description of activity changes in the four categories as follows: general activity, burst structure, synchronicity, and oscillatory behavior. Changes in general activity parameters describe the effects on action potential firing rate (spike rate), burst rate, and burst period as the time between the bursts. Burst structure parameters define not only the internal structure of spikes within a high-frequency spiking phase (burst), e.g., spike frequency in bursts, spike rate in bursts, and burst spike density, but also the overall structure of the burst, such as duration, area, and plateau. Oscillatory parameters quantify the regularity of occurrence or structure of bursts, which is calculated by coefficients of variation of primary activity parameters describing the variability of parameters (general activity, burst structure) within experimental episodes (31). Higher values indicate less regular burst structure or less regular general activity (e.g., spiking, bursting). As a measure of synchronicity in the spike trains, CVnet parameters reflect synchronization among neurons within the network (31). CVnet is the coefficient of variation over the network. Large CVnet values imply a wide range of variation in the activity across the network, meaning less synchronization. Twelve out of 204 parameters were visualized as the most describing ones divided into the four categories as follows: general activity, burst structure, oscillation, and synchronization. The definitions for these 12 parameters are as follows: spike rate: number of spikes per second, averaged over all spike trains recorded per 60 s bin; burst rate: number of bursts per second, a measure for burstiness of units, averaged over all units recorded per 60 s bin; spike contrast: describes the occurrence or absence of spikes in neighboring time segments of the spike train, reflecting the variability in burstiness of units within experimental episodes; burst duration: mean lengths of bursts (milliseconds) based on ISI method; burst amplitude: bursts are mathematically superimposed with an integral function. The integral is defined by spike peak density in bursts and number of spikes. Burst amplitude is the peak amplitude of the integrated burst reflecting the fraction of the bursts with highest spike density; burst spike density: mean frequency of spikes within bursts (Hertz), defined by the average of all interspike intervals in a burst. Burst spike density increases if the number of spikes in burst increases or burst duration decreases; burst rate SD: SD of burst rate across 60 s bins, indicating the variability of burstiness of units within temporal episodes; Syn All: average distance of bursts within a population burst from population burst center, a measure for the strength of synchronicity of a network; Syn share: average fraction of units involved in population bursts, with higher values reflecting a higher degree of synchronicity between the units; burst rate CVnet: coefficient of variation of burst rate, reflecting spatial variation of burst rate over the network during experimental episodes; event rate: number of burst events per second, with an event defined as synchronous burst activity of at least 50% of all units in a network within a time frame of 300 ms; hamming factor: or hamming distance between two spike trains is the number of positions at which corresponding burst events are different. Here, the hamming factor is calculated for all corresponding spike trains with a binning of 10 s.

Cross Validation and Similarity Analysis

Training data sets with all 204 spike train parameters were calculated for control and treatment groups. The respective data records of the two groups (exposure treatment and control) were classified using methods of pattern recognition (software package PatternExpert, NeuroProof GmbH, Rostock, Germany). As previously describes (26, 32), an artificial neuronal network was trained with the data using a multi-layer feed forward perceptron neural network and back propagation algorithm without hidden units and a resilient-propagation learning algorithm. There were as many input knots as there were parameters (204) and 4 output nodes, 1 for each classified group. Non-usage of hidden layers was justified by the relatively high variation of the data. The performed cross-validation indicates the functional similarity/dissimilarity of the treatment group and the control. χ^2 analysis was performed on the cross-validation data to test for significant effects.

Immunocytochemistry

The recorded cortical cultures on Axion 12-well MEAs, as well as concurrently cultured cortical networks on 24-well plates with 11 mm glass cover slips from the different treatment groups were further analyzed by immunocytochemistry, fluorescence microscopy, and semi-automatic quantitative image analysis. The cells were initially washed with PBS and fixed with 4% paraformaldehyde for 30 min, followed by the addition of a PBS-based blocking solution containing 1% BSA, 2% goat serum, and 0.05% TWEEN20. Cells were immunostained with primary antibodies for neurites with anti-tubulin beta-III (1:750; Sigma-Aldrich, Germany), neuronal soma with anti-Hu C/D (1:500; neuronal-specific RNA-stabilizing protein present in neuronal cell bodies) (Invitrogen, Germany), synapses with anti-synapsin-1 (1:200; Cell Signaling, Germany), GABAergic neurons with anti-GABA (1:500; Sigma-Aldrich), and nuclei with the DNA dye Hoechst/Bisbenzimide (1 µg/ml; Sigma-Aldrich, Germany). Cortical networks were embedded with Prolong antifade gold (LifeTechnologies, Germany) and analyzed with an upright fluorescence microscope (Nikon Eclipse E800, Nikon AG, Japan). Images were analyzed using a semi-automatic image quantification tool (ImageJ2x, Rawak Software, NIH, USA). The following parameters were quantified per image: cell number, neuron number, neurite number, synapse number, % neurons, neurites per neuron, synapses per neurite, and number of GABAergic neurons.

Statistical Analysis

For the data and statistical analysis, all recorded networks in each treatment group were used with no exception.

Results from primary analysis are expressed as series means ± SEM. The absolute parameters' distributions were tested for normality. The level of significance after exposure treatment was assessed by using Student's t-test and $p < 0.05$ was considered statistically significant.
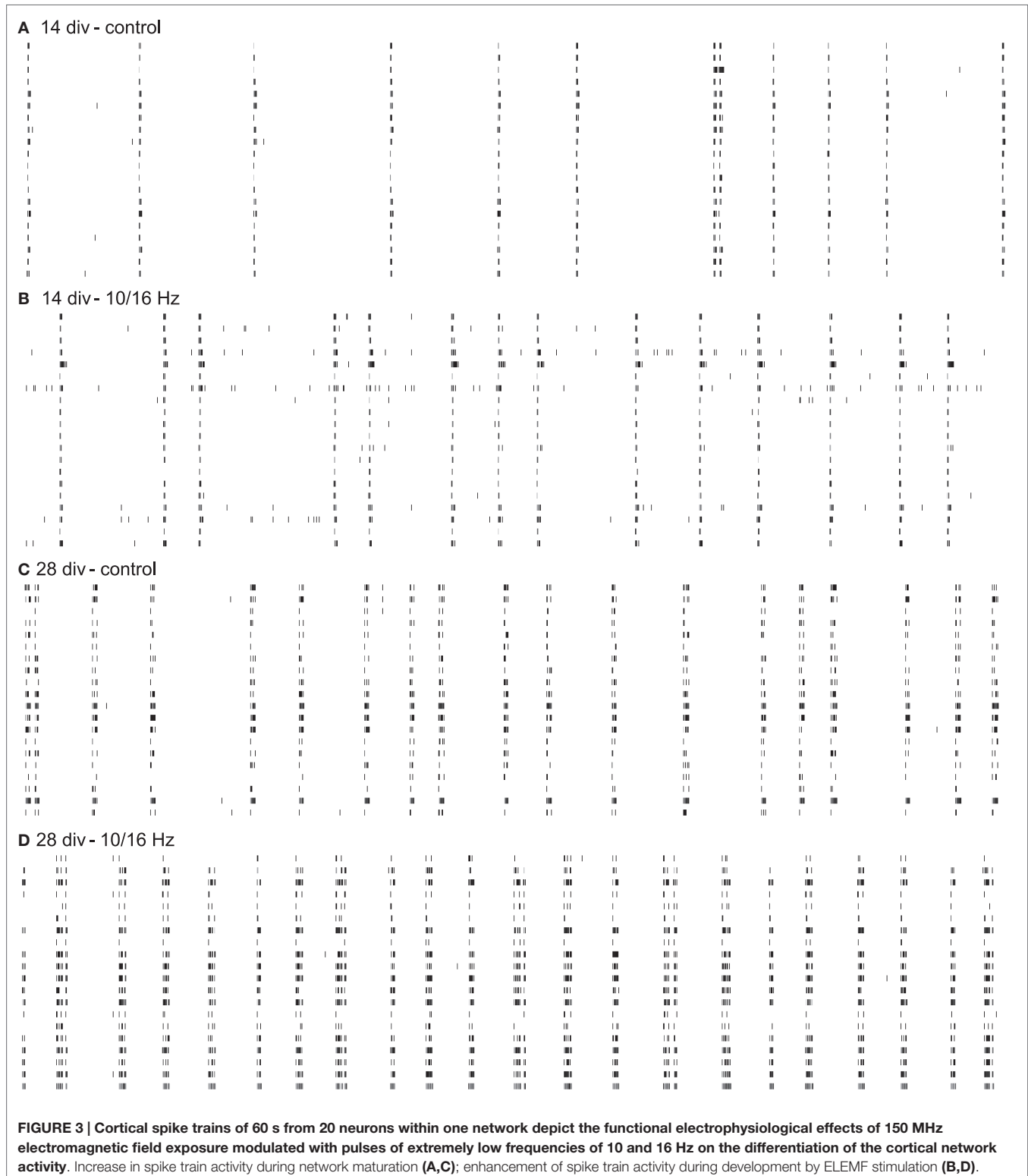
Results

In this study, we investigated the effects of electromagnetic exposure of an ELEMF with a 150 MHz carrier frequency, which was alternatingly modulated with 10 and 16 Hz, on the differentiation

of cortical networks' activity and morphology after 10 (14 div) and 24 days (28 div) of exposure. Therefore, we recorded the network activity as spike trains (**Figure 3**) and stained the cortical cultures for various morphological markers. We compared the effects of exposed and control condition.

Developmental Changes of the Cortical Network Activity and Morphology Under Control Conditions

Under control conditions, the development of the cortical network activity was characterized by a boost in general activity (**Figures 3A,C**). Here, from 14 to 28 div, the overall spiking and

FIGURE 3 | Cortical spike trains of 60 s from 20 neurons within one network depict the functional electrophysiological effects of 150 MHz electromagnetic field exposure modulated with pulses of extremely low frequencies of 10 and 16 Hz on the differentiation of the cortical network activity. Increase in spike train activity during network maturation **(A,C)**; enhancement of spike train activity during development by ELEMF stimulation **(B,D)**.

bursting activity increased approximately 3- and 2.5-fold. This is revealed by the increase in spike rate, burst rate, and the "spike contrast" to 317, 253, and 189%, respectively (**Figures 4A–C**). This activity enhancement was accompanied by a slight enlargement of burst structure with an increase in burst duration, burst amplitude, and burst spike density to 130, 106, and 106%, respectively (**Figures 4D–F**). The network pattern regularity remained unchanged during activity development (**Figures 4A–C**), as revealed by the unchanged spike and burst rate coefficients of variations over time (CVtime, data not shown). The increase in the spike rate SD was accompanied by an increase of the spike rate itself and the increase of the number of units recorded. The number of bursting units increased by 100% from 6 ± 1 to 12 ± 2 bursts per minute. A similar development was found for parameters reflecting the spiking and bursting synchronicity. The burst rate variation over the network (CVnet values) and the hamming factor were unaffected from 14 to 28 days (**Figures 4J–L**). Only the event rate increased over the network maturation to 213% due to the general increase in the spike and burst rate.

This cortical network activity enhancement was accompanied by changes in the morphology of the cortical neuron/glia co-culture (**Figure 5**). During the differentiation of the cortical networks between 14 and 28 div, the percentage of neurons increased from 19 ± 2 to $24 \pm 2\%$, whereas the total number of cells remained unaltered (**Figure 6**). The neurite density decreased by 29%. In addition, the percentage of GABAergic neurons increased from 19 ± 2 to $25 \pm 3\%$ (**Figure 6**).

Electromagnetic 150 MHz Exposure with 10 and 16 Hz Modulation Increased the Cortical Network Activity During the Process of Network Activity Maturation

At 14 div, after four treatments over the course of 10 days, the electromagnetic exposure caused an acceleration in the development of the network activity (**Figures 3A,B**). This is demonstrated by the increase in the general activity parameters spike rate, burst rate, and spike contrast to 155, 122, and 133%, respectively (**Figures 4A–C**). These general activity changes were accompanied by burst structure changes characterized by an elongation in burst duration to 130%, compared to control levels at 14 div (**Figures 4D–F**). The regularity and synchronicity of the network activity were not affected (**Figures 4G–L**).

The prolonged electromagnetic exposure (eight treatments over 24 days) over the cortical activity differentiation period of 28 days *in vitro*-induced activity changes of the same trend. The general activity was increased with respect to spike rate, and burst rate, and the spike contrast to 136, 123, and 116%, respectively. However, it was accompanied by reorganization within the burst structure (**Figures 3C,D**). While the burst duration was decreased to 81%, burst amplitude and burst spike density were increased to 129 and 137%. Also, the network patterns' synchronicity was increased, quantified by the increase in the event rate and the Hamming factor to 115 and 179%, respectively. Again, the network pattern regularity was not affected (**Figure 4**).

To further underpin the obtained results, all multiparametric spike train data sets of control and exposure groups at 14 and 28 div were further analyzed using pattern recognition. The cross-validation results of the classification revealed a good self-recognition of each data group and separation from the respective treatment or control groups (**Table 1**). About 76 and 71% of all data sets for 14 and 28 div cortical network activity recordings, respectively, recognized themselves correctly as control. In the ELEMF exposure groups, 56 and 59% of all data sets recognized themselves correctly and significantly as exposure group. Here, the diversity in percentage of correct recognition is due to the different size of data sets (=experiments per group) in the four groups. The χ^2 test, which considers the expectation value for each pattern recognition test, indicates significant effects.
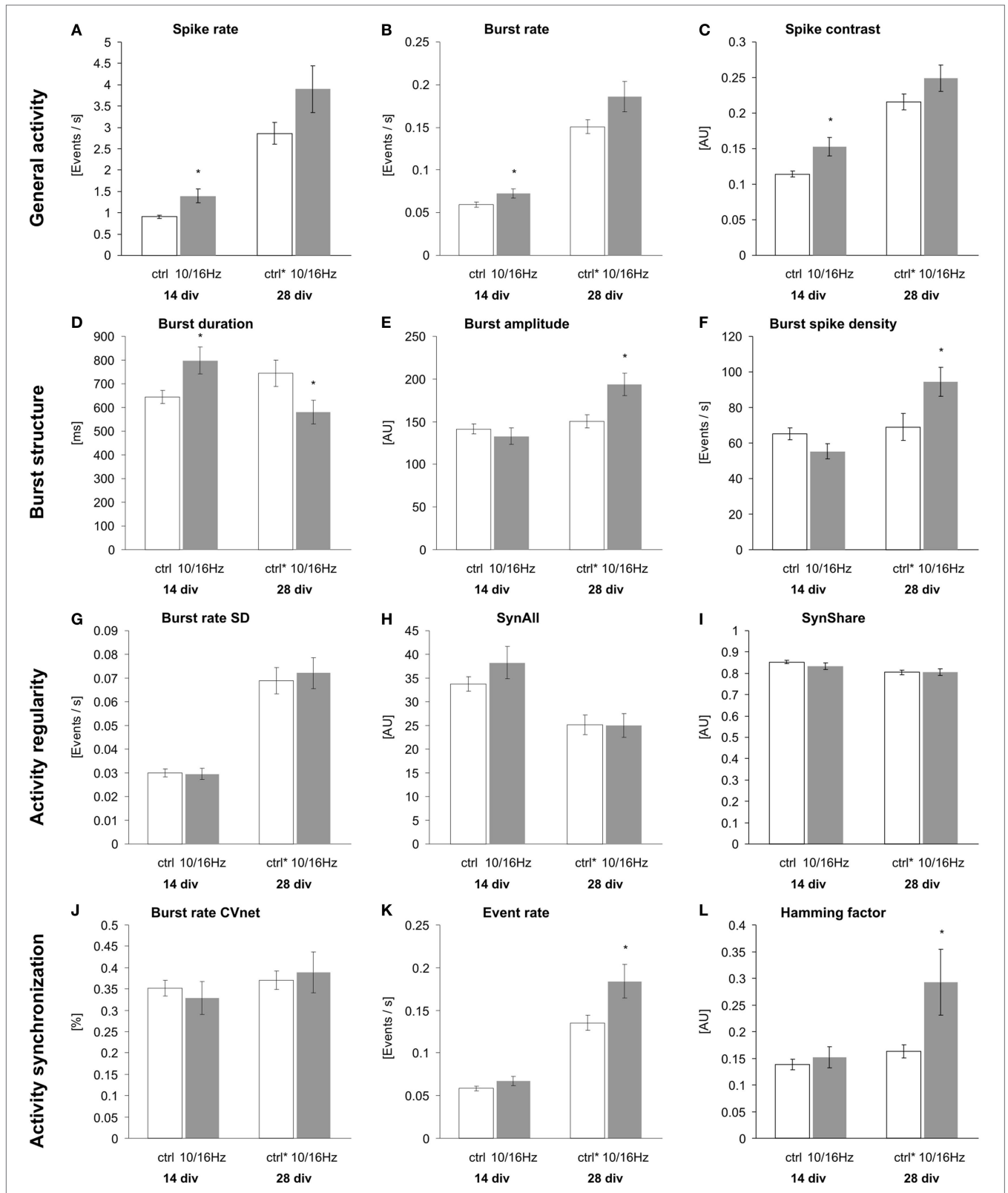
Effects of Electromagnetic Exposure on the Development of the Cortical Network Morphology

The repeated electromagnetic exposure with alternating 10 and 16 Hz frequency did not only influence the cortical network activity but also affected the development of the cortical network morphology (**Figure 5**). For a closer investigation of the mode of action, how the electromagnetic exposure changed the functional activity by either supporting neurogenesis, neuritogenesis, or synaptogenesis, the chronically treated cortical cultures on MEAs were fixed after recording to assess the cellular effects by immunocytochemistry. We quantitatively assessed synaptogenesis (synaptic puncta per image, per neuron), neuritogenesis (number of neurites/100 µm per image, per neuron), and neurogenesis (% neurons compared to non-neuronal cells), as well as the portion of GABAergic neurons by immunostaining for specific markers.

At 14 days *in vitro*, 10 days of repeated exposure induced an accelerated differentiation of cells into neurons, shown by an increase of neuronal somata by 11% with an unaltered total number of cells and accompanied increase of their ratio by 10% (**Figures 6A–C**). This is also underlined by an enhanced outgrowth of neurites to 113% (**Figure 6D**). The number of total synapses remained unaltered (**Figure 6E**), resulting in a decrease of the synaptic density (number of synapses per neurite) to 85% (**Figure 6F**). The staining of GABAergic cells revealed an increase in this specific neuronal population (**Figure 4G**) to 119%, while the unaffected ratio of GABAergic to total neuronal cell number (**Figure 4H**) indicates that the exposure induced an enhanced differentiation of a GABAergic neuronal subpopulation during early *in vitro* cortical cell culture differentiation.

These early effects of the alternating 10 and 16 Hz electromagnetic field exposure were largely compensated after 24 days of repeated exposure at div 28 (**Figure 6**). At this culture age, the differentiation is assumed to be completed; only the GABAergic neuronal subpopulation persisted at an increased level of 132% (**Figure 6G**).

To evaluate potential secondary effects of the ELEMF due to the platinum electrodes and conducting path in the MEA neurochip, we additionally analyzed the effects of the ELEMF stimulation of cortical networks on cover slips in 24-well plates. We chose 24-well over 12-well plates because their geometries provide culture conditions similar to the Axion 12-well MEAs considering cell density, total number of cells seeded, seeding area, and medium volume.

FIGURE 4 | Effects of 150 MHz electromagnetic field exposure pulse modulated with alternating 10 and 16 Hz on the differentiation of cortical network activity. Plotted are 12 activity-describing parameters from the multiparametric data analysis. The extracted parameters reflect the changes in the four activity categories general activity **(A–C)**, burst structure **(D–F)**, synchronization **(G–I)**, and oscillation **(J–L)**. Statistical significance is shown for the comparison between the control and the ELEMF group (mean ± SEM, Student's unpaired t-test: $*p \leq 0.05$; $**p \leq 0.01$; $***p \leq 0.001$).
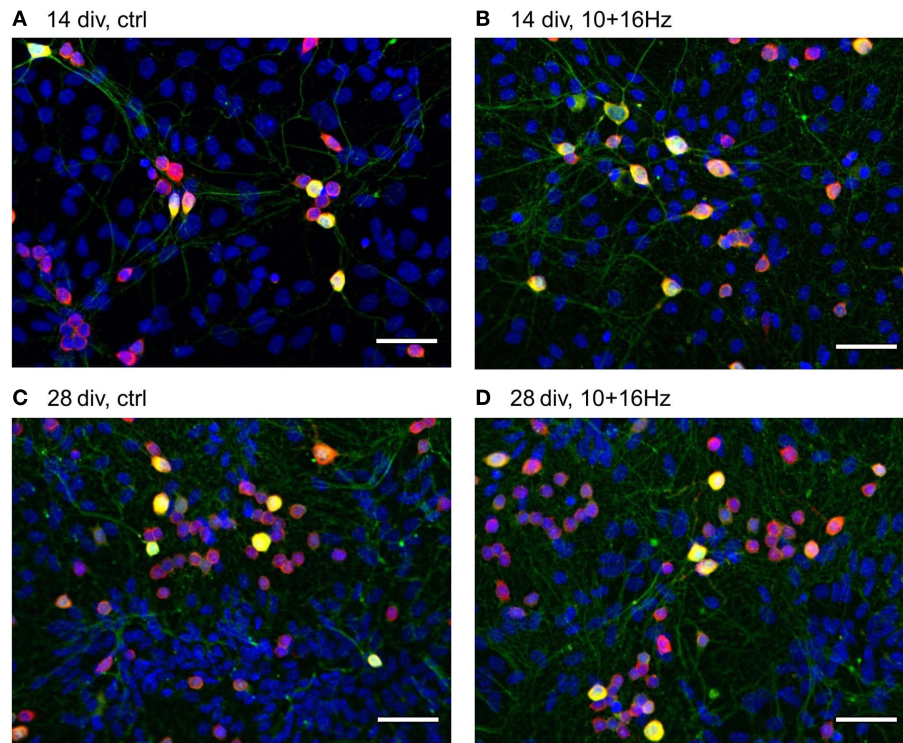
FIGURE 5 | Effects of 150 MHz electromagnetic field exposure pulse modulated with alternating 10 and 16 Hz on the development of cortical network morphology. Increase of total cell number, neurons, GABAergic neuronal subpopulation, and neurites during development from 14 to 28 div **(A,C)**; Additional increase in neurites and shift towards the neuronal population by ELEMF stimulation at 14 div **(B)** and shift to the GABAergic neuronal subpopulation by ELEMF stimulation at 14 and 28 div **(B,D)**. Color-merge of GABAergic neurons (green, anti-GABA), neuronal soma (red, anti-HuC/D), nuclei (blue, Hoechst), bar = 50 μm.

The cortical networks in 24-well plates revealed an increase of total number of neurons by 19% and an increase in the neuronal percentage by 22%. Here, the GABAergic population of neurons increased by 24% after 24 days of the ELEMF stimulation. These data are comparable to those obtained on the Axion 12-well chip. Hence, the effects were slightly higher than on the MEA chips, suggesting particular small counter effects induced by the electronics (electrodes and conducting paths) on the MEA chip.

Discussion

We demonstrated that the exposure of primary cortical *in vitro* networks with a 150 MHz carrier frequency, pulse modulated with alternating 10 or 16 Hz increased activity and intensified the burst structure within network activity. Overall, this effect was most pronounced already after 10 days of exposure at div 14. The development of cortical activity under these conditions was accelerated. These functional changes were accompanied by morphological ones. The effects on the morphological changes induced by the ELEMF stimulation on cortical networks in corresponding 24-well plates were higher compared to the effects induced in the networks on 12-well Axion chips. Yet, the percentage of neurons was increased with an unaffected total number of cells. This indicates an enhancement of neurogenesis or neuronal differentiation. The increase in neurites accompanied with a decrease of the synaptic density per neurites in the exposure group at 14 div also indicates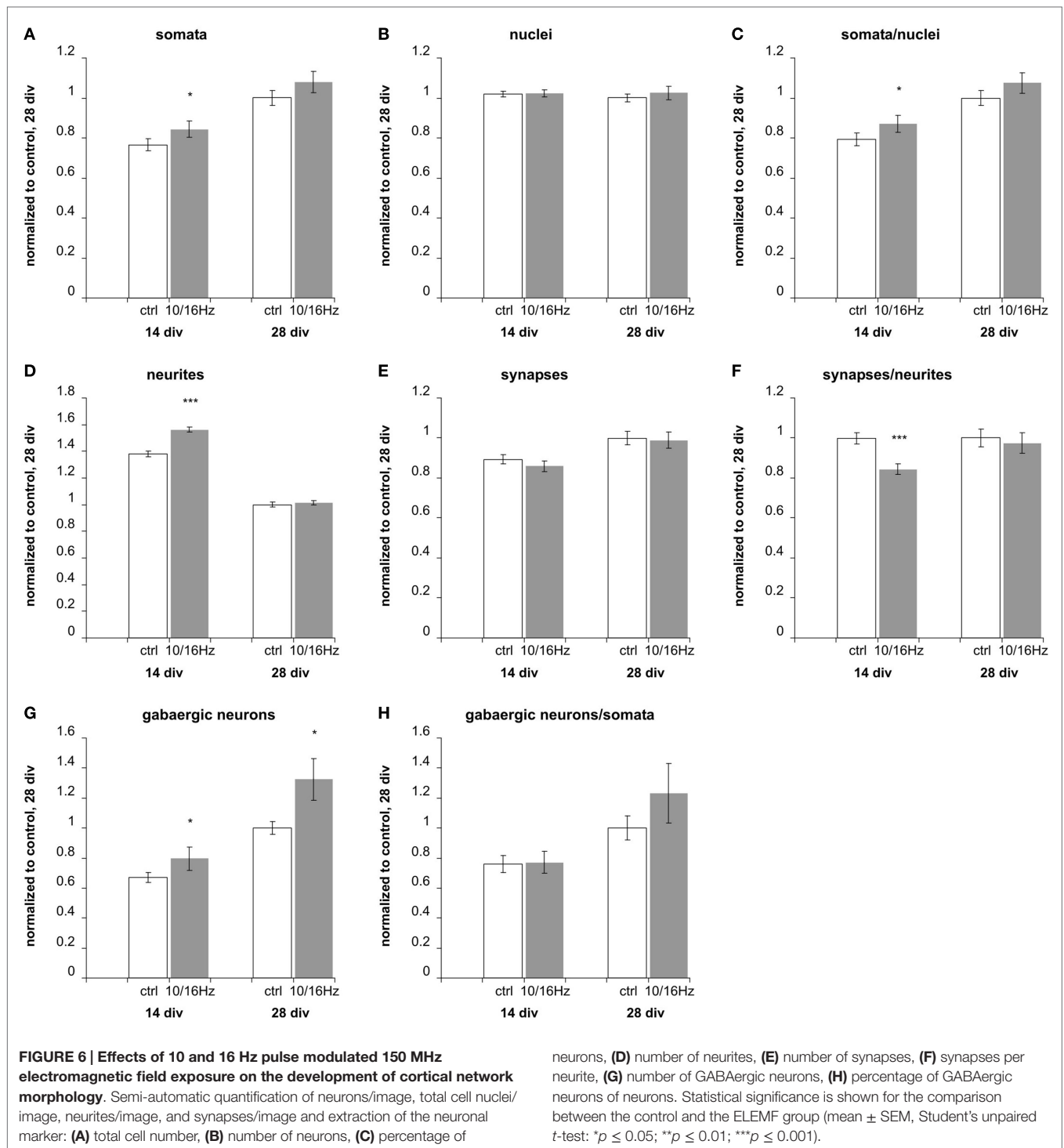 a prolonged synaptic plasticity by the ELEMF exposure. The electromagnetic stimulation selectively promoted the differentiation of neuronal populations, evident by the increased proportion of GABAergic neurons, which sustained a higher ratio after 24 days of stimulation at div 28. In contrast to studies where repeated pentylenetetrazole (PTZ) stimulation resulted in an increase in migrating neurons in hippocampus and induced seizure network activity (33, 34), the recordings of our cortical network activities showed no typical seizure activity at neither 14 nor 28 div.

In Alzheimer's disease (AD), numerous neurofibrillary tangles and Aβ plaques occur, and neurogenesis and neuronal plasticity are also markedly altered (35).

Therefore, much research effort has been devoted to identify stimuli capable of enhancing adult neurogenesis. Researchers provide evidence for one desirable outcome that can be attained via suitable magnetic fields, demonstrating an effective boost to rates of neurogenesis, the creation of new neurons in the brain. Higher rates of neurogenesis imply greater neuroplasticity, the ability of the brain to adapt, repair, and resist minor damage, which overall seems to be a good target to aim for.

Comparable to our *in vitro* approach the group around Adey demonstrated that ELEMF exposure (147 MHz, 6–20 Hz amplitude modulation) reinforced spontaneous brain rhythms in cats (36) as well as increasing the calcium efflux from chick cerebral tissue by more than 15% (37, 38). Due to the very high frequency of 150 MHz and the associated extreme slew rate of the device's pulse signals such a low value can still induce relatively high voltages

FIGURE 6 | Effects of 10 and 16 Hz pulse modulated 150 MHz electromagnetic field exposure on the development of cortical network morphology. Semi-automatic quantification of neurons/image, total cell nuclei/image, neurites/image, and synapses/image and extraction of the neuronal marker: **(A)** total cell number, **(B)** number of neurons, **(C)** percentage of neurons, **(D)** number of neurites, **(E)** number of synapses, **(F)** synapses per neurite, **(G)** number of GABAergic neurons, **(H)** percentage of GABAergic neurons of neurons. Statistical significance is shown for the comparison between the control and the ELEMF group (mean ± SEM, Student's unpaired t-test: *$p \leq 0.05$; **$p \leq 0.01$; ***$p \leq 0.001$).

(millivolts to 1 V) and currents (100 μA to 1 mA) in tissues or cells, which in turn may also have relevant physiological effects on the membrane potential or ionic currents of voltage-sensitive ion channels. Piacentini et al. (39) reported an increased expression and function of voltage-gated Ca^{2+} channels after exposure to ELEMFs whereat the Ca^{2+} influx through Ca(v)1 channels played a key role in promoting neuronal differentiation of murine neural stem/progenitor cells *in vitro*. In mice, ELEMFs *in vivo* promoted the proliferation and neuronal differentiation of hippocampal neural stem cells that functionally integrate in the dentate gyrus (40, 41) and enhanced newborn neuron survival *in vivo* (3.5 h/day for 6 days) (42). These alterations were associated with enhanced spatial learning and memory. Extremely low-frequency electrical or magnetic fields are thought to evoke changes in neuronal

TABLE 1 | Cross validation of exposure treatment group vs. control group: the activity profiles of the treatment groups at 14 and 28 div separate significantly from their respective control groups.

Day of recording	Data group	Control (%)	10 + 16 Hz (%)	χ^2 test (p value)
14 div	Control	76	24	
	10 + 16 Hz	44	56	0.0028
28 div	Control	71	29	
	10 + 16 Hz	41	59	0.0068

Values correspond to % of datasets of one group (rows) classified as either itself or the other group. The higher this value, the more distinct the functional profile is from each other. The statistical verification is performed by χ^2 test showing the separation of the datasets is statistically significant.

membrane potential at most in the microvolt range, which at first sight appear orders of magnitude too small to significantly influence neuronal signaling. However, a number of mechanisms in the central nervous system can amplify these signals, potentially allowing such small changes in membrane potential to induce significant physiological effects [for review, see Ref. (43)]. It has been reported that exposure to weak extremely low-frequency (ELF, 1–100 Hz) magnetic fields can influence brain electrical activity (EEG) in humans and animals (44, 45). Many behavioral effects have been reported for exposure to magnetic fields at different intensities, particularly with pulsed magnetic fields. The specific pulse form appears to be an important factor for the behavioral effects seen; for example, a pulsed magnetic field originally designed for spectroscopic MRI was found to alleviate symptoms in bipolar patients (46), while another MRI pulse had no effect. A whole-body exposure to a pulsed magnetic field was found to alter standing balance and pain perception in other studies (47, 48).

Given the role of stem cells, e.g., in hippocampal functions, such as cognition, and given their potential for brain repair, Fitzsimons et al. (49) reviewed the epigenetic mechanisms relevant for neuron stem cell proliferation and AD etiology. In this context, Robel et al. (50) discussed a new view on astrocyte-like reactive glia, as a suggested widespread endogenous source of cells with stem cell potential, which might potentially be harnessed for local repair strategies. Ma et al. (51) argued for a role of these glia cells in controlling multiple steps of adult neurogenesis, from proliferation and fate specification of neural progenitors to migration and integration of the neuronal progeny into pre-existing neuronal circuits in the adult brain and their potential function in degenerative neurological diseases, such as AD. These data are consistent with data presented here, where the ELEMF exposure-induced neurogenesis without affecting the total number of cells, which suggests that progenitor cells where differentiated into neurons instead to glial cells. Such enhanced differentiation into neurons seems to

be directed into the GABAergic neuron population. This could be important, because precisely timed neuronal activity across brain regions is crucial for cognitive processing (52) and, e.g., a division of GABAergic cell types is controlling network activities in hippocampus (53–55). Those GABAergic cells in a cell-type specific manner coordinate brain rhythm interactions. A slight change in the ratio of GABAergic cell types could result in diverse changes of electrical activity patterns in our cortical cultures.

Another hypothesis is that the ELEMF exposure could trigger alpha frequency bands in the brain, and induce similar changes as confirmed for neurofeedback training of the upper-alpha frequency band, improving cognitive enhancement (56–58). Rhythmic activity in the alpha band (8–13 Hz) is a core feature of cortical communication (59) and cognition (60) and was demonstrated in various studies to modulate neural firing (61), perceptual detection rates (62, 63), and cerebral blood flow (64). Alpha-band oscillations exert a critical influence on the excitability level of neocortical networks as well as on the timing of neuronal responses (59, 65). Alpha rhythms were also observed in thalamic neurons *in vitro* (66, 67). Electrophysiological *in vitro* recordings and computational models of thalamic circuits show that during strong phasic inhibition the spiking of relay-mode neurons and pyramidal cells are entrained by the phase of the alpha cycle (68, 69). Upper-alpha frequency is widely shown to be correlated with cognitive performance (70, 71). First clinical trials with the here applied ELEMF frequency exposure design on patients with mentally impaired perception revealed an improvement of their cognitive behavior after daily stimulation with 150 MHz with a pulsed 10 and 16 Hz modulation for 14 days; in this respect, in an ongoing clinical study, the effects of the ELEMF stimulation on diminution of beta-Amyloid deposition are tested [personal communication Prof. W. Pries].

In conclusion, the studies discussed above support the initial hypothesis that this kind of stimulation is not only a treatment option for specific diseases or indications but also a completely new therapeutic low-energy electromagnetic field approach with promising potential for CNS applications. Further detailed studies to elucidate the molecular mechanisms mediating the ELEMF effects might lead to the development of novel therapeutic approaches for degenerative diseases, such as AD.

References

1. Virchow R. Die Verbindung der Naturwissenschaften mit der Medizin. In: Virchow R, Sudhoff K, editors. *Rudolf Virchow und die deutschen Naturforscherversammlungen*. Leipzig: Akadem. Verlagsgesellschaft (1922). 261 p.
2. Adey WR. Biological effects of electromagnetic fields. *J Cell Biochem* (1993) **51**:410–6. doi:10.1002/jcb.2400510405
3. Adey WR. Potential therapeutic applications of nonthermal electromagnetic fields: ensemble organization of cells in tissue as a factor in biological field sensing. In: Rosch PJ, Markov M, editors. *Bioelectromagnetic Medicine*. New York, NY: Marcel Dekker (2004). p. 1–16.
4. Markov M. Pulsed electromagnetic field therapy history, state of the art and future. *Environmentalist* (2007) **27**:465–75. doi:10.1007/s10669-007-9128-2
5. Pilla A, Fitzsimmons R, Muehsam D, Wu J, Rohde C, Casper D. Electromagnetic fields as first messenger in biological signaling: application to calmodulin-dependent

signaling in tissue repair. *Biochim Biophys Acta* (2011) **1810**:1236–45. doi:10.1016/j.bbagen.2011.10.001

6. Pilla AA. Nonthermal electromagnetic fields: from first messenger to therapeutic applications. *Electromagn Biol Med* (2013) **32**:123–36. doi:10.3109/15368378.2013.776335

7. Del Seppia C, Ghione S, Luschi P, Ossenkopp KP, Choleris E, Kavaliers M. Pain perception and electromagnetic fields. *Neurosci Biobehav Rev* (2007) **31**:619–42. doi:10.1016/j.neubiorev.2007.01.003

8. Taylor EM, Hardy KL, Alonso A, Pilla AA, Rohde CH. Pulsed electromagnetic fields dosing impacts postoperative pain in breast reduction patients. *J Surg Res* (2014) **153**(1):504–10. doi:10.1016/j.jss.2014.08.007

9. Blanchard JP, Blackman CF. Clarification and application of an ion parametric resonance model for magnetic field interactions with biological systems. *Bioelectromagnetics* (1994) **15**:217–38. doi:10.1002/bem.2250150306

10. Blackman CF, Blanchard JP, Benane SG, House DE. The ion parametric resonance model predicts magnetic field parameters that affect nerve cells. *FASEB J* (1995) **9**:547–51.

11. Simko M. Cell type specific redox status is responsible for diverse electromagnetic field effects. *Curr Med Chem* (2007) **14**:1141–52. doi:10.2174/092986707780362835

12. Bassett CA, Pawluk RJ, Pilla AA. Acceleration of fracture repair by electromagnetic fields. A surgically noninvasive method. *Ann N Y Acad Sci* (1974) **238**:242–62. doi:10.1111/j.1749-6632.1974.tb26794.x

13. Pilla AA. Electrochemical information transfer at living cell membranes. *Ann N Y Acad Sci* (1974) **238**:149–70. doi:10.1111/j.1749-6632.1974.tb26785.x

14. Binhi VN, Goldman RJ. Ion-protein dissociation predicts 'windows' in electric field-induced wound-cell proliferation. *Biochim Biophys Acta* (2000) **1474**:147–56. doi:10.1016/S0304-4165(00)00002-7

15. Hosomi K, Kishima H, Oshino S, Hirata M, Tani N, Maruo T, et al. Cortical excitability changes after high-frequency repetitive transcranial magnetic stimulation for central poststroke pain. *Pain* (2013) **154**:1352–7. doi:10.1016/j.pain.2013.04.017

16. Hosomi K, Shimokawa T, Ikoma K, Nakamura Y, Sugiyama K, Ugawa Y, et al. Daily repetitive transcranial magnetic stimulation of primary motor cortex for neuropathic pain: a randomized, multicenter, double-blind, crossover, sham-controlled trial. *Pain* (2013) **154**:1065–72. doi:10.1016/j.pain.2013.03.016

17. Maruo T, Hosomi K, Shimokawa T, Kishima H, Oshino S, Morris S, et al. High-frequency repetitive transcranial magnetic stimulation over the primary foot motor area in Parkinson's disease. *Brain Stimul* (2013) **6**:884–91. doi:10.1016/j.brs.2013.05.002

18. Pries W, Baumgart D. *Effektivität der Befeldungstherapie (Hochfrequenz-Zellresonanztherapie) mit 150 MHz/Modulation 10 Hz bei erwachsenen Patienten mit Kniegelenksarthrose* (2006). Available from: http://www.dgeim.de/page5/page81/studie2_effektivitaet.pdf

19. Butcher EC. Can cell systems biology rescue drug discovery? *Nat Rev Drug Discov* (2005) **4**:461–7. doi:10.1038/nrd1754

20. Swinney DC, Anthony J. How were new medicines discovered? *Nat Rev Drug Discov* (2011) **10**:507–19. doi:10.1038/nrd3480

21. Swinney DC. Phenotypic vs. target-based drug discovery for first-in-class medicines. *Clin Pharmacol Ther* (2013) **93**:299–301. doi:10.1038/clpt.2012.236

22. Gross GW, Harsch A, Rhoades BK, Gopel W. Odor, drug and toxin analysis with neuronal networks in vitro: extracellular array recording of network responses. *Biosens Bioelectron* (1997) **12**:373–93. doi:10.1016/S0956-5663(97)00012-2

23. Stett A, Egert U, Guenther E, Hofmann F, Meyer T, Nisch W, et al. Biological application of microelectrode arrays in drug discovery and basic research. *Anal Bioanal Chem* (2003) **377**:486–95. doi:10.1007/s00216-003-2149-x

24. Xia Y, Gross GW. Histiotypic electrophysiological responses of cultured neuronal networks to ethanol. *Alcohol* (2003) **30**:167–74. doi:10.1016/S0741-8329(03)00135-6

25. Gramowski A, Jügelt K, Stüwe S, Schulze R, McGregor GP, Wartenberg-Demand A, et al. Functional screening of traditional antidepressants with primary cortical neuronal networks grown on multielectrode neurochips. *Eur J Neurosci* (2006) **24**:455–65. doi:10.1111/j.1460-9568.2006.04892.x

26. Gramowski A, Jügelt K, Schroeder OH, Weiss DG, Mitzner S. Acute functional neurotoxicity of lanthanum(III) in primary cortical networks. *Toxicol Sci* (2011) **120**:173–83. doi:10.1093/toxsci/kfq385

27. Johnstone AF, Gross GW, Weiss DG, Schroeder OH, Gramowski A, Shafer TJ. Microelectrode arrays: a physiologically based neurotoxicity testing platform for the 21st century. *Neurotoxicology* (2010) **31**:331–50. doi:10.1016/j.neuro.2010.04.001

28. Novellino A, Scelfo B, Palosaari T, Price A, Sobanski T, Shafer TJ, et al. Development of micro-electrode array based tests for neurotoxicity: assessment of interlaboratory reproducibility with neuroactive chemicals. *Front Neuroeng* (2011) **4**:4. doi:10.3389/fneng.2011.00004

29. Gramowski A, Stüwe S, Jügelt K, Schiffmann D, Loock J, Schroeder O, et al. Detecting neurotoxicity through electrical activity changes of neuronal networks on multielectrode neurochips. *ALTEX* (2006) **22**:410–5.

30. Weiss DG. Neurotoxicity assessment by recording electrical activity from neuronal networks on microelectrode array neurochips. In: Aschner M, Sunol C, Price AB, editors. *Cell Culture Techniques*. New York: Humana Press, c/o Springer Science + Business Media (2011). 467 p.

31. Gramowski A, Jügelt K, Weiss DG, Gross GW. Substance identification by quantitative characterization of oscillatory activity in murine spinal cord networks on microelectrode arrays. *Eur J Neurosci* (2004) **19**:2815–25. doi:10.1111/j.0953-816X.2004.03373.x

32. Schultz L, Zurich MG, Culot M, Fabulas-da Costa A, Landry C, Bellwon P, et al. Evaluation of drug-induced neurotoxicity based on metabolomics, proteomics and electrical activity measurements in complementary CNS in vitro models. *Toxicol In vitro* (2015) **S0887-2333**(15):120–24. doi:10.1016/j.tiv.2015.05.016

33. Buga AM, Vintilescu R, Balseanu AT, Pop OT, Streba C, Toescu E, et al. Repeated PTZ treatment at 25-day intervals leads to a highly efficient accumulation of doublecortin in the dorsal hippocampus of rats. *PLoS One* (2012) **7**:e39302. doi:10.1371/journal.pone.0039302

34. Schmoll H, Badan I, Grecksch G, Walker L, Kessler C, Popa-Wagner A. Kindling status in Sprague-Dawley rats induced by pentylenetetrazole: involvement of a critical development period. *Am J Pathol* (2003) **162**:1027–34. doi:10.1016/S0002-9440(10)63897-7

35. Blanchard J, Wanka L, Tung YC, Cardenas-Aguayo Mdel C, Laferla FM, Iqbal K, et al. Pharmacologic reversal of neurogenic and neuroplastic abnormalities and cognitive impairments without affecting Abeta and tau pathologies in 3xTg-AD mice. *Acta Neuropathol* (2010) **120**:605–21. doi:10.1007/s00401-010-0734-6

36. Bawin SM, Gavalas-Medici RJ, Adey WR. Effects of modulated very high frequency fields on specific brain rhythms in cats. *Brain Res* (1973) **58**:365–84. doi:10.1016/0006-8993(73)90008-5

37. Bawin SM, Adey WR, Sabbot IM. Ionic factors in release of 45Ca2+ from chicken cerebral tissue by electromagnetic fields. *Proc Natl Acad Sci U S A* (1978) **75**:6314–8. doi:10.1073/pnas.75.12.6314

38. Bawin SM, Sheppard A, Adey WR. Possible mechanisms of weak electromagnetic field coupling in brain tissue. *Bioelectrochem Bioenerg* (1978) **5**:67–76. doi:10.1016/0302-4598(87)87008-3

39. Piacentini R, Ripoli C, Mezzogori D, Azzena GB, Grassi C. Extremely low-frequency electromagnetic fields promote in vitro neurogenesis via upregulation of Ca(v)1-channel activity. *J Cell Physiol* (2008) **215**:129–39. doi:10.1002/jcp.21293

40. Cuccurazzu B, Leone L, Podda MV, Piacentini R, Riccardi E, Ripoli C, et al. Exposure to extremely low-frequency (50 Hz) electromagnetic fields enhances adult hippocampal neurogenesis in C57BL/6 mice. *Exp Neurol* (2010) **226**:173–82. doi:10.1016/j.expneurol.2010.08.022

41. Leone L, Fusco S, Mastrodonato A, Piacentini R, Barbati SA, Zaffina S, et al. Epigenetic modulation of adult hippocampal neurogenesis by extremely low-frequency electromagnetic fields. *Mol Neurobiol* (2014) **49**:1472–86. doi:10.1007/s12035-014-8650-8

42. Podda MV, Leone L, Barbati SA, Mastrodonato A, Li Puma DD, Piacentini R, et al. Extremely low-frequency electromagnetic fields enhance the survival of newborn neurons in the mouse hippocampus. *Eur J Neurosci* (2014) **39**:893–903. doi:10.1111/ejn.12465

43. Mathie A, Kennard LE, Veale EL. Neuronal ion channels and their sensitivity to extremely low frequency weak electric field effects. *Radiat Prot Dosimetry* (2003) **106**:311–6. doi:10.1093/oxfordjournals.rpd.a006365

44. Tattersall JE, Scott IR, Wood SJ, Nettell JJ, Bevir MK, Wang Z, et al. Effects of low intensity radiofrequency electromagnetic fields on electrical activity in rat hippocampal slices. *Brain Res* (2001) **904**:43–53. doi:10.1016/S0006-8993(01)02434-9

45. Bell GB, Marino AA, Chesson AL, Struve FA. Human sensitivity to weak magnetic fields. *Lancet* (1991) **338**:1521–2. doi:10.1016/0140-6736(91)92336-Z

46. Rohan M, Parow A, Stoll AL, Demopulos C, Friedman S, Dager S, et al. Low-field magnetic stimulation in bipolar depression using an MRI-based stimulator. *Am J Psychiatry* (2004) **161**:93–8. doi:10.1176/appi.ajp.161.1.93

47. Thomas AW, White KP, Drost DJ, Cook CM, Prato FS. A comparison of rheumatoid arthritis and fibromyalgia patients and healthy controls exposed to a pulsed (200

microT) magnetic field: effects on normal standing balance. *Neurosci Lett* (2001) **309**:17–20. doi:10.1016/S0304-3940(01)02009-2

48. Shupak NM, Prato FS, Thomas AW. Human exposure to a specific pulsed magnetic field: effects on thermal sensory and pain thresholds. *Neurosci Lett* (2004) **363**:157–62. doi:10.1016/j.neulet.2004.03.069

49. Fitzsimons CP, Van Bodegraven E, Schouten M, Lardenoije R, Kompotis K, Kenis G, et al. Epigenetic regulation of adult neural stem cells: implications for Alzheimer's disease. *Mol Neurodegener* (2014) **9**:25. doi:10.1186/1750-1326-9-25

50. Robel S, Berninger B, Gotz M. The stem cell potential of glia: lessons from reactive gliosis. *Nat Rev Neurosci* (2011) **12**:88–104. doi:10.1038/nrn2978

51. Ma DK, Ming GL, Song H. Glial influences on neural stem cell development: cellular niches for adult neurogenesis. *Curr Opin Neurobiol* (2005) **15**:514–20. doi:10.1016/j.conb.2005.08.003

52. Singer W. Neurobiology. Striving for coherence. *Nature* (1999) **397**(391):393. doi:10.1038/17024

53. Klausberger T, Magill PJ, Marton LF, Roberts JD, Cobden PM, Buzsaki G, et al. Brain-state- and cell-type-specific firing of hippocampal interneurons in vivo. *Nature* (2003) **421**:844–8. doi:10.1038/nature01374

54. Tukker JJ, Fuentealba P, Hartwich K, Somogyi P, Klausberger T. Cell type-specific tuning of hippocampal interneuron firing during gamma oscillations in vivo. *J Neurosci* (2007) **27**:8184–9. doi:10.1523/JNEUROSCI.1685-07.2007

55. Bienvenu TC, Busti D, Magill PJ, Ferraguti F, Capogna M. Cell-type-specific recruitment of amygdala interneurons to hippocampal theta rhythm and noxious stimuli in vivo. *Neuron* (2012) **74**:1059–74. doi:10.1016/j.neuron.2012.04.022

56. Zoefel B, Huster RJ, Herrmann CS. Neurofeedback training of the upper alpha frequency band in EEG improves cognitive performance. *Neuroimage* (2011) **54**:1427–31. doi:10.1016/j.neuroimage.2010.08.078

57. Escolano C, Olivan B, Lopez-del-Hoyo Y, Garcia-Campayo J, Minguez J. Double-blind single-session neurofeedback training in upper-alpha for cognitive enhancement of healthy subjects. *Conf Proc IEEE Eng Med Biol Soc* (2012) **2012**:4643–47. doi:10.1109/EMBC.2012.6347002

58. Nan W, Rodrigues JP, Ma J, Qu X, Wan F, Mak PI, et al. Individual alpha neurofeedback training effect on short term memory. *Int J Psychophysiol* (2012) **86**:83–7. doi:10.1016/j.ijpsycho.2012.07.182

59. Jensen O, Mazaheri A. Shaping functional architecture by oscillatory alpha activity: gating by inhibition. *Front Hum Neurosci* (2010) **4**(4):186. doi:10.3389/fnhum.2010.00186

60. Vanrullen R, Koch C. Visual selective behavior can be triggered by a feed-forward process. *J Cogn Neurosci* (2003) **15**:209–17. doi:10.1162/089892903321208141

61. Haegens S, Nacher V, Luna R, Romo R, Jensen O. Alpha-oscillations in the monkey sensorimotor network influence discrimination performance by rhythmical inhibition of neuronal spiking. *Proc Natl Acad Sci U S A* (2011) **108**:19377–82. doi:10.1073/pnas.1117190108

62. Varela FJ, Toro A, John ER, Schwartz EL. Perceptual framing and cortical alpha rhythm. *Neuropsychologia* (1981) **19**:675–86. doi:10.1016/0028-3932(81)90005-1

63. Dugue L, Marque P, Vanrullen R. The phase of ongoing oscillations mediates the causal relation between brain excitation and visual perception. *J Neurosci* (2011) **31**:11889–93. doi:10.1523/JNEUROSCI.1161-11.2011

64. Scheeringa R, Fries P, Petersson KM, Oostenveld R, Grothe I, Norris DG, et al. Neuronal dynamics underlying high- and low-frequency EEG oscillations contribute independently to the human BOLD signal. *Neuron* (2011) **69**:572–83. doi:10.1016/j.neuron.2010.11.044

65. Klimesch W, Sauseng P, Hanslmayr S. EEG alpha oscillations: the inhibition-timing hypothesis. *Brain Res Rev* (2007) **53**:63–88. doi:10.1016/j.brainresrev.2006.06.003

66. Jahnsen H, Llinas R. Electrophysiological properties of guinea-pig thalamic neurones: an in vitro study. *J Physiol* (1984) **349**:205–26. doi:10.1113/jphysiol.1984.sp015154

67. Jahnsen H, Llinas R. Ionic basis for the electro-responsiveness and oscillatory properties of guinea-pig thalamic neurones in vitro. *J Physiol* (1984) **349**:227–47. doi:10.1113/jphysiol.1984.sp015154

68. Lorincz ML, Kekesi KA, Juhasz G, Crunelli V, Hughes SW. Temporal framing of thalamic relay-mode firing by phasic inhibition during the alpha rhythm. *Neuron* (2009) **63**:683–96. doi:10.1016/j.neuron.2009.08.012

69. Vijayan S, Kopell NJ. Thalamic model of awake alpha oscillations and implications for stimulus processing. *Proc Natl Acad Sci U S A* (2012) **109**:18553–8. doi:10.1073/pnas.1215385109

70. Klimesch W. EEG alpha and theta oscillations reflect cognitive and memory performance: a review and analysis. *Brain Res Brain Res Rev* (1999) **29**:169–95. doi:10.1016/S0165-0173(98)00056-3

71. Klimesch W. Alpha-band oscillations, attention, and controlled access to stored information. *Trends Cogn Sci* (2012) **16**:606–17. doi:10.1016/j.tics.2012.10.007